

방사성 폐기물 처분장에서의 열응력에 의한 암반균열 팽창 및
투수율 변화에 관한 연구

Potential for fracture shear slip due to
thermo-mechanical loading of a deep geological
repository for nuclear waste

Ki-Bok Min(민기복) (서울대학교)

Ove Stephansson(GeoForschungsZentrum, Germany)

1. Introduction

A field investigation by Barton et al. (1995) supports the contention that critically stressed fractures are the ones that carry the major portion of the fluid flow and this finding was demonstrated numerically by Min et al. (2004). While characterizing permeability is one of the most important tasks in determining the feasibility of geological repository for nuclear waste, it is important to recognize that the fluid-carrying ability of underground rock, i.e., its permeability, is a dynamic variable over the lifespan of a geological repository (Rutqvist and Stephansson, 2003).

The objective of the current study is to examine the contribution of thermal stress to the shear slip and permeabilities of fractured rocks in mid- and far-field around the repository,

2. Methodology

This study is composed of three steps as shown in Figure 1. In the first step, three-dimensional thermomechanical analysis is conducted to obtain the full stress history in the far-field around the repository. The analysis use COMSOL MULTIPHYSICS which is a flexible partial differential equation solver that uses the finite element method (COMSOL, 2008). Equations of heat conduction and elasticity are coupled and the modified code was verified against a known thermo-elastic solution (Timoshenko and Goodier, 1970). In the second stage, stress history obtained from the first stage is used to establish the boundary conditions for the DFN-DEM (Discrete Fracture Network-Discrete Element Method) approach (Min et al., 2004). DFN is constructed at selected points in mid- and far-field based on the site investigation data from Forsmark (Glamheden, 2006). For the DEM calculations, two-dimensional distinct element code, UDEC, is used for this study (Itasca, 2006). Finally, the third stage is devoted to integration of outcomes from the first and second stages to quantify the shear slip potential and corresponding permeability changes.

3. THERMOMECHANICAL ANALYSIS

3.1 Geometry and Geological Data

All deposition holes and tunnels were lumped as a thin rectangular plate of uniform thickness and the size of the square was calculated considering the number of canisters, the spacing of

deposition holes and the separation between the deposition tunnels (Brantberger et al., 2006). The equivalent side length and the thickness of the repository was calculated to be 1.2 km and 13.3 m, respectively, and the size of the model was 2 km x 2 km x 0.8 km (depth). Monitoring points of variables are shown in Figure 1. Heat decay data from the canister, rock properties, in-situ stress and initial temperature data were from the site investigations (Glamheden, 2007).

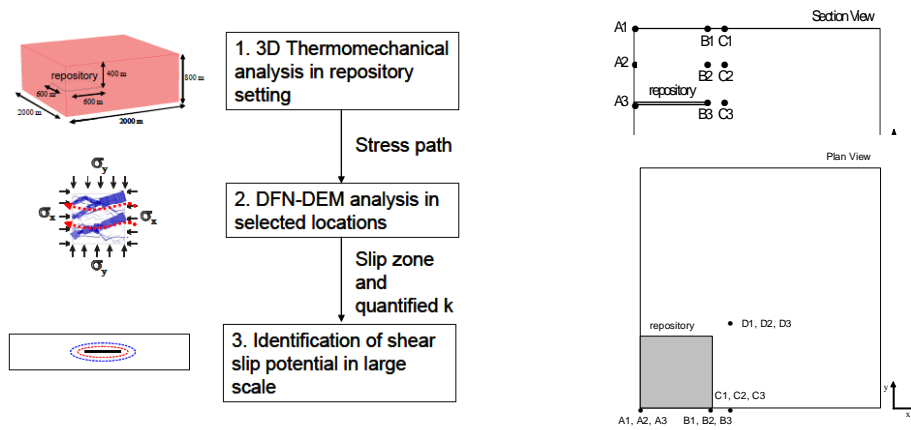


Figure 1. Three components of the modeling work and monitoring points around repository.

3.2 Temperature evolution

Temperature evolutions in selected locations and temperature distributions are plotted in Figure 2. The maximum temperature was around 42°C in the vicinity of the repository after 100-500 years. At mid-depth monitoring points, which were at a depth of 200 m below ground surface, the maximum temperature was barely higher than 20°C (except right above the repository, A2), and the maximum temperature at this depth was achieved at around 1,000 years.

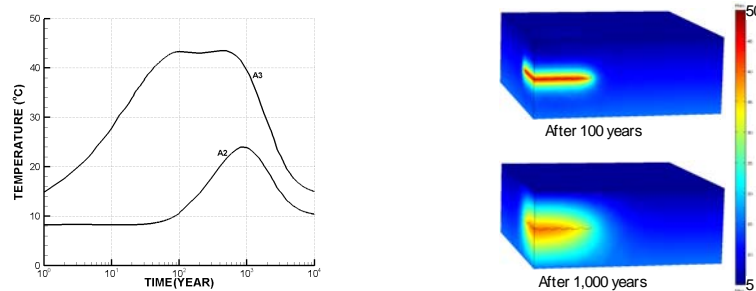
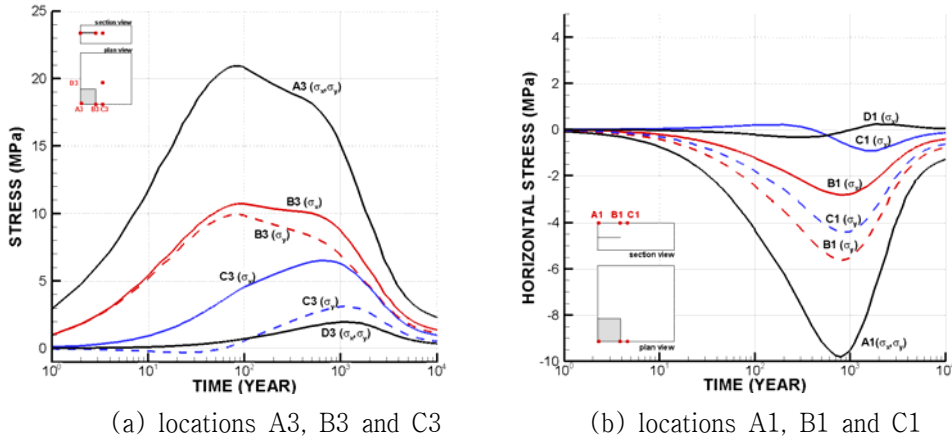


Figure 2. Temperature evolutions at locatins A2 and A3 and temperature distribution.

3.3 Thermal Stress Evolutions

Figure 3(a) shows the evolution of stresses in the horizontal direction at various points at the repository level. The maximum compressive stress of 20 MPa was observed at the center of the repository after about 100 years. At the periphery of the repository the magnitudes were smaller, with a maximum compressive stress of about 10 MPa. Maximum horizontal compressive stress was observed in the center of the repository at repository level and horizontal stresses were isotropic. Also, notable anisotropic horizontal compressive stresses were observed near the periphery of the repository.



(a) locations A3, B3 and C3

(b) locations A1, B1 and C1

Figure 3 Evolution of thermal stresses at selected points

The time for maximum compressive stress to occur varied from 100 years to 1,000 years, depending on the locations of the monitoring points. Figure 3(b) shows that significant tensile stresses developed at locations A1, B1 and C1 at the ground surface above the repository. The maximum tensile stress was in the order of 10 MPa at the surface right above the center of the repository. The maximum tensile stresses were observed at the ground surface, and the time for maximum tensile stress was about 1,000 years. Transition from tensile to compressive stress occurred at about the mid-depth point right above the repository (A2 and B2). While tensile stresses near the surface were oriented horizontally, vertical tensile stresses were observed at the repository level in the vicinity of the repository (C3 and D3).

Figure 4 shows the transition of stress state plotted in terms of Mohr Circle at locations A3 and A1. The friction coefficients of fractures used for upper and lower bounds were 1.0 and 0.6, respectively. In location A3, which is located at a depth of 400 m, the possibility of failure greatly increases after 100 years due to the comparatively high horizontal stress. After 1,000 years, the contribution of thermal stress to the failure of fracture is less significant due to the relatively homogeneous increase of thermal stress. A different mechanism dominated the fracture failure mode at location A1, which is located at the surface. Because of the high horizontal tensile thermal stress, on the order of 10 MPa, fractures were prone to tensile failure, e.g., after 1,000 years, as shown by solid-red circles in Figure 4. It is important to note that this tensile failure is expected much later in time than the previous shear failure.

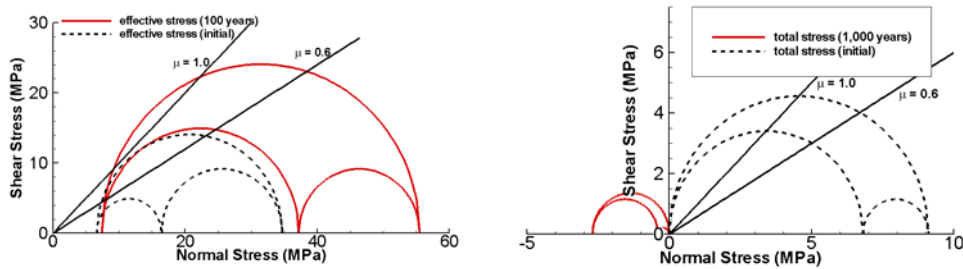


Figure 4 State of stress at location A3 (left) and A1 (right).

Figure 5 illustrates thermally-induced horizontal compressive stresses, tensile stresses and shear stresses observed in the setting of a deep geological repository. It is noted that all three modes of stresses can increase the shear slip potential in one way or another. Importantly, the slips occur at different times. Increased horizontal compressive stress enhances the possibility of shear slip because of the remaining constant vertical stress component. Anisotropic horizontal compressive stress can increase the shear slip potential depending on the anisotropy of the horizontal component of in-situ stress (Figure 5(a)). Horizontal tensile stress reduces high total horizontal stress and can act in reducing the shear slip potential. However, generation of significant tensile stress, up to 10 MPa at the surface, can cause tensile failure of sealed fractures. Vertical tensile stresses generated at the periphery of the repository at the repository level reduce the total vertical stress and this increases the probability of shear slip (Figure 5(b)). Thermally-induced generation of shear stress can contribute to the rotation of principal stress and can increase the shear slip potential of shallow dipping and near vertical fractures (Figure 5(c)). More detailed accounts with actual analyses can be found at Min and Stephansson (2009).

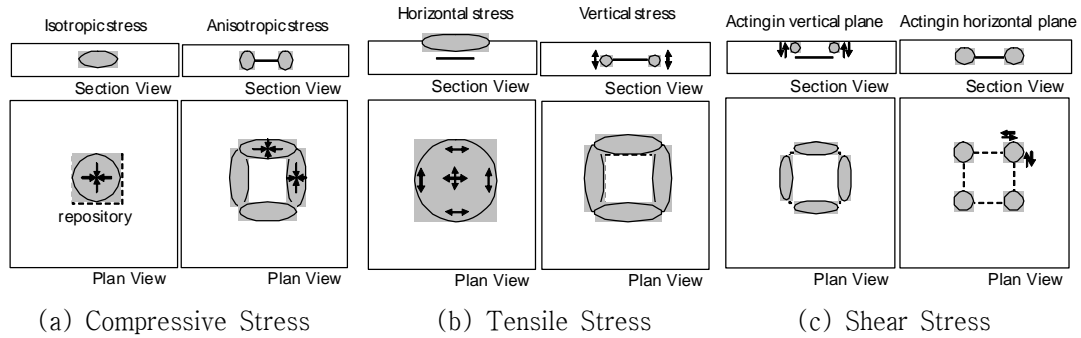


Figure 5 Classified regions of thermal stress change during the operation of a repository.

4. DFN–DEM ANALYSIS

4.1 Methodology

DFN-DEM analysis uses the discrete fracture network (DFN) as the geometry of the fractured rock and applies the discrete element method (DEM) for the analysis of mechanical and hydraulic behaviours (Min et al., 2004). For the generation of DFN, a two dimensional DFN generator was used and UDEC (Universal Distinct Element Code) was used for the DEM calculation (Itasca, 2006). Ten 5 m by 5 m DFN models were generated using the DFN generator in order to represent a more general behavior of fracture rock mass. Intact rock and fracture properties for the DEM calculation are from the site investigation at Forsmark (Glamheden et al., 2007).

4.2 Permeability change during a cycle of heating and cooling

Permeability measurements were conducted on six models of DFN using two sets of stress paths at selected locations. The selected locations were A3 and C3 at the repository level for which a reasonable possibility of shear slip and permeability increase were expected. Final stresses

were calculated by superimposing the generated thermal stress on in-situ stress. Figure 6 shows the final stress path used for the numerical experiment. Figure 7 shows the permeability and flow rates change due to the stress changes from heating for a DFN. The major mechanism of permeability change in four out of six of the models (DFN3, DFN6, DFN7, DFN10) was normal deformation (closure) of fractures without shear slip. This can be explained by the lack of optimally oriented fractures with respect to the stress orientation and poor connectivity in these models. Only two models (DFN5 and DFN9) showed shear slip and permeability increases up to a factor of four.

An interesting observation is the non-reversibility of the permeability for the time scale of 10,000 years. Unlike the models for which normal closure dominated, permeability did not recover in the two models in which shear slip was a dominant mechanism. This demonstrates the importance of irreversibility of permeability once shear slip does occur. Vertical permeability at the repository level was insensitive to stress changes due to the fact that vertical fractures were largely closed at this magnitude of stress.

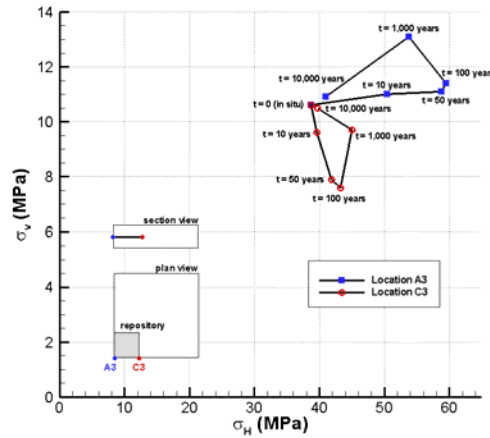


Figure 6 Stress path during the thermal history at monitoring point A3 and C3.

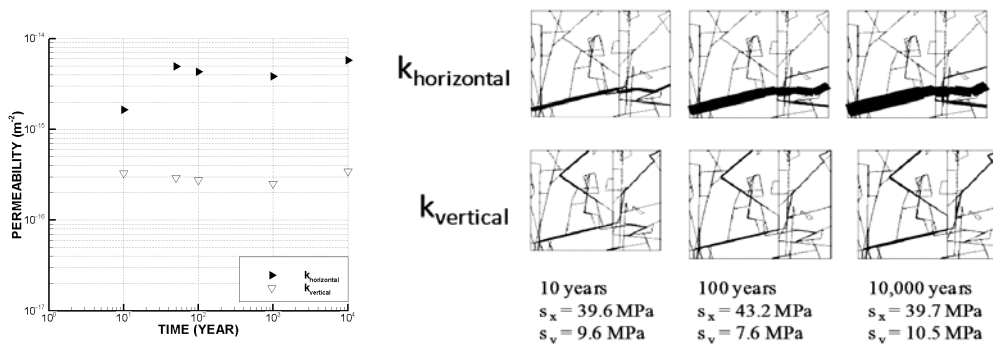


Figure 7 Permeability and flow rates evolutions at monitoring point C3 (DFN5).

5. CONCLUSIONS

In this study, the zones of fracture shear slip were examined by conducting a three-dimensional

thermo-mechanical analysis of a repository model. Stress evolutions in selected locations showed the main mechanisms of the generation of thermal stress, which were important for fracture shear slip as summarized in Figure 5.

The implications of these mechanisms are that fractures of different orientations are vulnerable to shear slip at various locations in and around a deep geological repository. While the main mechanism was comparatively large horizontal stresses, tensile and shear thermal stresses are also expected to contribute to the opening of fractures.

DFN-DEM analyses of six DFN models at the repository level showed that normal deformation dominated fracture closure/opening in four models and shear dilation dominated in the remaining two models. In the latter two models, modest increases of permeability, up to a factor of four, were observed during thermal loading history.

Permeability change caused by shear dilation was not recovered after cooling of the repository. This is explained by the irreversible fracture shear deformation after failure, which is in contrast with the recovered permeability for models where normal fracture closure dominates.

Finally, analysis in this study was conducted on the data from the Forsmark site, Sweden, and this analysis has implications for sites that have comparatively large horizontal in-situ stresses.

ACKNOWLEDGEMENTS

This work was supported by SSM (Swedish Radiation Safety Authority) through the INSITE (INdependent Site Investigation Tracking and Evaluation) group of SSM.

REFERENCES

1. Barton, C.A., Zoback, M.D. & Moos, D. 1995. Fluid-flow along potentially active faults in crystalline rock. *Geology*, 23(8):683-686.
2. Brantberger, M. et al., 2006. Final repository for spent nuclear fuel. Underground design Forsmark, Layout D1. SKB R-06-34.
3. Comsol, 2008. Comsol Multiphysics® Ver 3.5 Reference Manual.
4. Glamheden, R., Fredriksson, A., Röshoff, K., Karlsson, J., Hakami, H. & Christiansson, R. 2007. Rock Mechanics Forsmark site descriptive modeling Forsmark stage 2.2, SKB R-07-31.
5. Itasca Consulting Group. 2006. Universal Distinct Element Code manual, Ver 4.0.
6. Min, K.-B., Rutqvist, J., Tsang, C.-F. & Jing, L. 2004. Stress-dependent permeability of fractured rock masses: a numerical study, *Int J Rock Mech & Min Sci*, 41(7):1191-1210.
7. Rutqvist, J. & Stephansson, O. 2003. The role of hydromechanical coupling in fractured rock engineering. *Hydrogeology Journal*, 11:7-40.
8. Timoshenko, S.P. & Goodier, J.N. 1970. *Theory of Elasticity*, 3rd Edition, McGraw-Hill Book Co.
9. Min K.-B., Stephansson O., 2009, Shear-induced Fracture Slip and Permeability change - implications for long-term performance of a deep geological repository, SSM Report, 2009:xx